

FACTA UNIVERSITATIS

Series: **Electronics and Energetics** Vol. 32, N° 1, March 2019, pp. 51-63

<https://doi.org/10.2298/FUEE1901051D>

REDUCTION OF SUSCEPTIBILITY FROM ELECTROMAGNETIC INTERFERENCE IN SENSORLESS FOC OF IPMSM *

Lindita Dhamo¹, Aida Spahiu¹, Mitja Nemec², Vanja Ambrozič²

¹Polytechnic University of Tirana, Faculty of Electrical Engineering, Tirana, Albania

²University of Ljubljana, Faculty of Electrical Engineering, Ljubljana, Slovenia

Abstract: *This paper presents main problems of practical implementation of Field Oriented Control (FOC) developed for an Interior Permanent Magnet Synchronous Motor (IPMSM). The main sources of Electromagnetic Interferences (EMI) noises are discussed and practical aspects when a position sensor is used are presented. The control system is based on the DSP processing unit, together with inverter and encoder. The main problem addressed in this paper is reduction of vibrations in torque and speed response in a real system by re-placing a hardware device of control system very susceptible to EMI noises, like encoder, with a soft block in control unit like Sliding Mode Observer, less sensitive to EMI. The experimental results with this control structure show considerable ripple reduction at steady state in torque, speed and current, as a consequence of reduction of sensitivity to EMI noises.*

Key words: EMI, IPMSM, sensorless FOC.

1. INTRODUCTION

PMSM has become really competitive to an induction motor in terms of lifetime cost. This motor has recently become quite attractive due to its many advantages because magnets, instead of windings, are used for rotor magnetization [2]. Phase inductance of PMSM is lower than that of the induction motor. Thus, in PMSM, the effect of electromagnetic noise is greater when compared to the induction motor [3].

Electro Magnetic Interference (EMI), the appropriate term when referring to lower frequencies, or Radio Frequency Interference (RFI), the appropriate term when referring to higher frequencies, is unwanted electrical noise that can interfere with signaling or communication equipment. Drives with 8 kHz or higher switching frequency have many harmonic frequencies, which produce problematic emissions affecting sensitive equipment.

Received February 3, 2018; received in revised form October 12, 2018

Corresponding author: Aida Spahiu

Polytechnic University of Tirana, Faculty of Electrical Engineering, Sheshi "Nene Tereza" Nr.4, 1000, Tirana, Albania (E-mail: aida.spahiu@fie.upt.al)

*An earlier version of this paper was presented at the 13th International Conference on Applied Electromagnetics (IIEC 2017), August 30 - September 01, 2017, in Niš, Serbia [1].

Reducing the PWM carrier frequency reduces the effects and lowers the risk of common mode noise interference. Higher carrier frequencies are less efficient for the drive, but lower carrier frequencies are less efficient for the motor. In general, restricting the propagation of electrical noise as close to the noise source as possible is the best way to protect sensitive devices from EMI.

There are many studies about the reduction of EMI on AC drive systems. Random PWM technique has been developed to suppress EMI in power converters [4]–[8] and have shown that with this method it is possible to reduce acoustic noise and mechanical vibration. Random PWM are various carried out in ways, such as by random switching frequency, random pulse position technique and random switching technique. It was shown that acoustic noise and EMI were suppressed by using random PWM technique in SVPWM algorithm [9]–[10]. Methods having various switching frequencies like random or chaotic PWM are generally applied to induction motor. Chaotic signal is obtained more easily than the random signal and it is also simpler to apply [11]. Various techniques are available and discussed in literature, such as Chaotic sinusoidal PWM, Chaotic pulse position PWM, hybrid chaotic SPWM and chaotic SV-PWM methods [12]–[14].

EMI can create adverse effects with electrical components in the motor control panel, contributing to a loss of serial communication, nuisance drive trips and disturbance of control signals. EMI not only degrades the performance of electrical equipment but also decreases the lifetime of components and increases the financial cost for equipment maintenance.

This paper deals with electromagnetic interference (EMI) and its prevention through the design of control system. It present the case when the sensitive device from EMI, or noise receiver, is replaced with a soft block in control scheme, less sensitive to EMI, in order to reduce the negative effect of EMI propagation that are present in the system.

2. MATHEMATICAL MODEL OF AN IPMSM WITH SYSTEM UNCERTAINTIES

2.1 Dynamic Model of an IPMSM

Applying Kirchhoff's voltage law (KVL) to the dq-axis equivalent circuits of a three-phase IPMSM yields the following voltage equations in the synchronously rotating d-q reference frame:

$$V_{qs} = R_s i_{qs} + L_{qs} \dot{i}_{qs} + \omega L_{ds} i_{ds} + \omega \lambda_m \quad (1)$$

$$V_{ds} = R_s i_{ds} + L_{ds} \dot{i}_{ds} - \omega L_{qs} i_{qs} \quad (2)$$

where V_{ds} and V_{qs} are the dq-axis voltages, i_{ds} and i_{qs} are the dq-axis currents, R_s is the stator resistance, L_{ds} and L_{qs} are the dq-axis inductances, ω is the electrical rotor speed, and λ_m is the magnetic flux.

In addition, the electromagnetic torque can be obtained from the following electrical and mechanical equations:

$$T_e = \frac{3}{2} \frac{p}{2} [\lambda_m i_{qs} + (L_{ds} - L_{qs}) i_{ds} i_{qs}] \quad (3)$$

$$T_e = T_L + B \frac{2}{p} \omega + J \frac{2}{p} \dot{\omega} \quad (4)$$

where T_e and T_L are the electromagnetic and load torques, p is the number of pole pairs, B is the viscous friction coefficient, and J is the rotor inertia.

Substituting (3) into (4) yields the following speed dynamic equation:

$$\dot{\omega} = \frac{3}{2} \frac{p^2}{4} \frac{\lambda_m}{J} i_{qs} - \frac{B}{J} \omega - \frac{p}{2J} T_L + \frac{3}{2} \frac{p^2}{4} \frac{L_{ds} - L_{qs}}{J} i_{ds} i_{qs} \quad (5)$$

2.2 The extraction of rotor position

The extraction of rotor position is made using the magnitudes of the $\alpha\beta$ back EMF components and inverse tangent method. In this method the rotor position angle is determined from as follows:

$$\hat{\theta} = \tan^{-1} \left(\frac{\hat{e}_\alpha}{\hat{e}_\beta} \right) \quad (6)$$

However, the position calculated by this method depends on the quality of the estimated back EMF. Because of the low sampling frequency, the estimated back EMF will have both phase and magnitude shifts, which will bring oscillations and phase shift to the estimated position. In order to mitigate the oscillation of the estimated position, an estimated speed feedback algorithm is used to improve the inverse tangent method for position calculation, as shown in Fig. 2, and the formula is as (7).

$$\hat{\theta}_2[k] = \hat{\theta}[k-1] + \omega[k-1] \cdot T_s \quad (7)$$

Block diagram that represent the algorithm for improving the inverse tangent method for rotor position calculation is shown in figure 2. There is a logic used for rotor position selection, which consist in comparison of evaluated position during the k^{th} time step, of $\hat{\theta}_1[k]$ that can be obtained from the SMO, and $\hat{\theta}_2[k]$ that has been calculated at the end of the $(k-1)^{\text{th}}$ time step. The error $\varepsilon[k]$ between $\hat{\theta}_1[k]$ and $\hat{\theta}_2[k]$ will be calculated as difference of them at the beginning of the k^{th} time step. If the generated error $\varepsilon[k]$ is smaller than the predetermined position error margin, than $\hat{\theta}[k] = \hat{\theta}_1[k]$; otherwise, $\hat{\theta}[k] = \hat{\theta}_2[k]$. This method used to extract the rotor position, in implementation has shown a good performance of speed control for IPMSM and the oscillations in the estimated rotor position are mitigated.

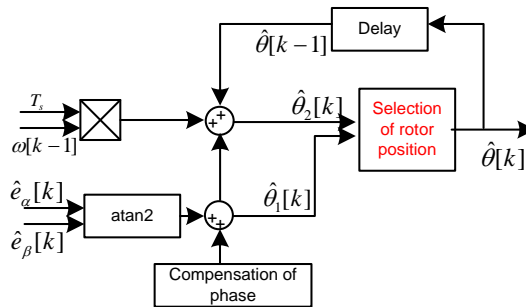


Fig. 2 Block diagram to improve the inverse tangent method for position calculation.

3. EMI NOISES AND EFFECTS

The reasons for electromagnetic compatibility (EMC) having grown in importance at such a rapid pace are owed to the increasing frequency because of use of digital electronics in today's world and the virtually worldwide imposition of governmental limits on the radiated and conducted noise emissions of digital electronic products [15]. There are three ways to prevent interference: suppress the emission at its source, make the coupling path as inefficient as possible, make the receptor less susceptible to the emission. Although these three alternatives should be kept in mind, the "line of defense" in this work is to make the receptor less susceptible to the emission. The paper shows the effect of replacing a device of the control system (the absolute en-coder) with a soft block (Sliding Mode Observer) into control scheme, in order to reduce the disturbances caused by EMI. The experimental results confirm the effectiveness of sensorless Field Oriented Control by Sliding Mode Observer of IPMSM in decreasing the sensitivity of control system to EMI noises.

3.1. EMI noise transmission path

Each type of interference problem includes a source, a receptor, and a transmission path between the source and victim or receptor of noise that suffer from EMI noises.

Conducted EMI is defined as interference that uses conductors as a path from a source to receptor. For example, a motor encoder grounded to a noisy connection would conduct noise to the drive encoder interface. The conducted noise could cause the drive encoder interface to receive inexact voltage signals precluding the motor drive from reading the rotor position and speed correctly thus causing drive faults. At the beginning, it may be supposed that the root cause for the drive operational malfunctions are related to incorrect parameter setting or possibly a faulty drive interface board. Closer inspection reveals the culprit to be poor grounding of the encoder cable.

Radiated EMI is defined as interference that uses a wireless path from a source to the receptor. This is commonly seen in motor control panels with AC motor wires are laid in parallel next to low-voltage control wiring. The result is coupling between the wires causing disturbances on the data transmission line. For example, if the motor wires were laid in close proximity to a serial link between the motor controller and the drive, the coupling of the signals may corrupt the data packets being transferred between the controller and drive.

3.2. EMI noise sources

The motor drive system (MDS) in industrial applications has become a new noise source because its switching frequency, operation voltage and current variations have been increased, causing unwanted effects such as common-mode (CM) noise and electromagnetic interference (EMI) [16]. Hence, the analysis of the noise propagation paths is necessary for understanding and improving the system reliability. Noise propagation paths are mainly composed of an inverter, a three phase cable, a ball-bearing, an electric motor, and multiple ground nodes. Especially the electric motor is an electric active load of inverter and a mechanical power source of vehicle as well. Therefore, unwanted current flows to whole vehicle body through the electric motor by capacitive coupling in both the electric components and the mechanical parts.

EMC of electronic circuits is to a great extent determined by the way the components are laid out and inter-connected. Signal lines with their corresponding return line form an antenna, which is able to radiate electromagnetic energy, where the magnitude is determined by current amplitude, frequency and the geometrical area of the current loops. There are three typical sources for EMI: power supply lines, signal lines carrying high frequency, oscillator circuit.

An important source of electromagnetic interference noise is the crosstalk. This essentially refers to the unintended electromagnetic coupling between wires and PCB lands that are in close proximity. Crosstalk is distinguished from antenna coupling in that it is a near-field coupling problem. Crosstalk between wires in cables or between lands on PCBs concerns the intrasystem interference performance of the product; that is, the source of the electro-magnetic emission and the receptor of this emission are within the same system. Thus this reflects the third concern in EMC: the design of the product such that it does not interfere with itself. With clock speeds and data transfer rates in digital control systems steadily increasing, crosstalk between lands on PCBs is becoming a significant mechanism for interference in modern digital systems.

3.3. Receptors of EMI

In a real digital control system, there are several devices sensitive to EMI, like encoders, tachometers, analog signals and measurement devices, communication networks and devices, microprocessor devices etc. Each of them demonstrates specific symptoms when affected by EMI noises. Encoders may include jumping around of encoder counts when still and non-repeatable positioning when moving. Tachometers may include incorrect speed reporting or un-expected speed fluctuations. Analog signals and measurement devices may include unexpected voltage spikes, ripple, or jitter on the analog signal causing incorrect and non-repeatable readings. Communication networks and devices almost always include loss of communication or errors in reading or writing data. The microprocessor devices can include loss of communications, faults or failure in the processor, digital inputs or outputs to trigger unexpectedly, analog inputs or outputs to report the incorrect value. The upper devices are all very important and irreplaceable, except the encoder. In the sensorless control system that we have developed, the elimination of one of the most sensitive receiver noises from EMI, will reduce significantly the negative effects, like ripple in analog signals: torque, speed and current. In this paper, the effect of replacing the en-coder with an observer of sliding mode type is investigated.

4. IPMSM SENSORLESS CONTROL

4.1. Control unit

The control system for sensorless FOC of IPMSM with Sliding Mode Observer, developed in this study, is composed by three main blocks: control unit, power module and measurement unit. The control unit is based upon a Piccolo F28069 controlstick DSP by TI [17]. It consists of an ADC converter, PWM channels and floating point central processing unit. The stator windings of IPMSM are supplied from a conventional 3 phase power module made up of 6 MOSFET-s, operated as keys for break control.

4.2. Measurement unit

The measurement unit is a determinative part in the closed loop control system and encoder has a crucial role since the performance of FOC depends directly on accurate rotor position information. In this study, only the effect of encoder in EMI noises is considered. The idea has been realized through a soft block added in control unit block. Instead of absolute encoder a Sliding Mode Observer to calculate the rotor position and rotor speed that are needed for FOC algorithm is designed. The results for important quantities of control system are then compared.

4.3. Modular philosophy of Digital Motor Control

Although a standardized platform, a modular TI Piccolo F28069 controlstick DSP provides a smooth way for customers to quickly port the reference software to customized hardware. TI's modular philosophy, which clearly separates modules into CPU and peripheral-dependent (drivers) categories, greatly simplifies the porting process. The IPMSM speed controller and the speed calculator from position information is the appropriate partitioning point in this system due to its complexity and reusability. This modular philosophy of TI's platforms has encouraged and allowed us to develop and modify the standard DMC system to a sensorless one. The figure 1 shows an overall block diagram of the proposed observer-based nonlinear sliding mode speed control system.

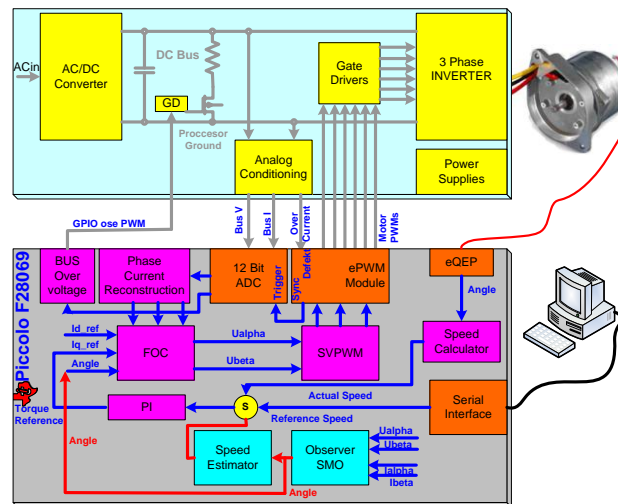


Fig. 1 Control scheme of sensorless SMO IPMSM drive.

The blocks “Speed estimator” and “Observer SMO” are added in the existing control scheme in order to calculate the rotor position and rotor speed through voltages and currents of stator, digitized and transformed by Clarke Transformation (to u_α , u_β , i_α and i_β) skipping the need for encoder, that gives a very important information like rotor position. The control scheme, by a soft-key provides sensed or sensorless operation and experimental results for quantities like torque, speed and currents to be compared and analyzed.

5. EXPERIMENTAL SETUP

In order to verify the performance and effectiveness in EMI noise reduction of the proposed observer-based non-linear sliding mode controller, experiments are carried out with a prototype IPMSM drive system based on a Piccolo F28069 controlstick DSP. Figure 2 shows the Experimental setup of sensorless SMO IPMSM drive. The hardware circuit consists of an IPMSM, product of Slovenian industry MAHLE-Letrika dedicated for electric power steering systems, a three-phase inverter with 6 MOSFETs (IRFP4410), a control board with a F28069 controlstick DSP (float-point), an absolute optical encoder (Hengstler AD35, 22 bit), two Hall-Effect current sensors (LTS15NP), and a PMSM motor as load in a back-to-back configuration. Table 1 show the parameters of IPMSM used in experiment.

The dc-link voltage (295 VDC) is obtained from the utility (AC 230V/50Hz) using a single-phase full-bridge rectifier. The two phase currents (i_a , i_b) are measured by LTS15-NP Hall Sensors and then converted into digital form using two 12-bit A/D converters. In addition, the rotor position (θ), which is used to execute the coordinate transformation for FOC, is measured by the absolute encoder and fed to Texas Instruments Piccolo F28069 controlstick DSP via a 32-bit QEP. Note that the rotor speed (ω) required to perform the feedback control can be easily obtained by differentiating θ with respect to time.

Table 1 IPMSM Parameters.

Parameters	Symbol	Unit	Value
Rated power	P_n	W	600
Rated speed	ω_n	rpm	1250
Stator resistance	R_s	Ω	0.06
d-axis Inductance	L_d	mH	0.068
q-axis Inductance	L_q	mH	0.086
Total linkage flux	λ_{PM}	Wb	0.0373
Pole pairs	p		3
Inertia	J	kgm ²	0.0001682

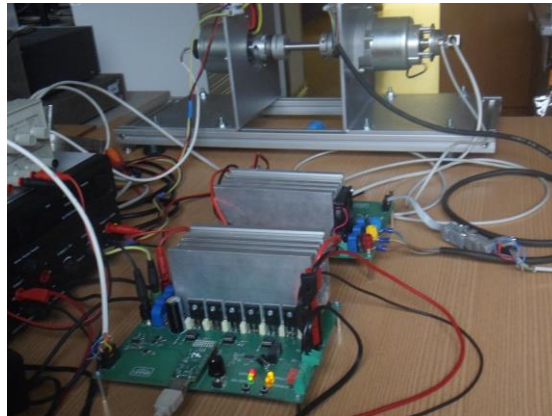


Fig. 2 Experimental setup of sensorless SMO of IPMSM drive.

6. EXPERIMENTAL RESULTS AND DISCUSSIONS

A variety of experiments have been performed. Results for sensor and sensorless mode are compared in order to evaluate the EMI noises reduction by replacing the absolute encoder with Sliding Mode Observer. Since the EMI noises are due to lot of complex and coupled factors, the effect of removing only the position sensor is checked in all electric and mechanic quantities that are important for the quality of control like torque, speed, and currents. That kind of nonlinear control used in our experiments, the Sliding Mode Control, “suffer” from chattering phenomena while implementation in real time control of IPMSM drive. It is obvious that the chattering is overlapped to speed and torque ripples, resulting in a worse situation. But the encoder, is the most susceptible hardware part of the drive by EMI, and replacing that hardware with a software, the SMO, reduce the possibility to effect the drive operation. Experimentally, result that the torque ripples are reduced up to 50%.

Furthermore, the existence of a no observable zone for very low speeds of motor is a weak point of operation for IPMSM drive . So the results for speed response in steady state are taken at two different regimes: for rated speed and low speed, 15 rev/s and 3.5 rev/s, respectively. The figures are presented in appropriate scale to compare the amplitudes of ripples for both sensor and sensorless operation (the reference signal is shown for speed).

Experimental results show that sensorless control exhibits less ripples in electromagnetic torque.

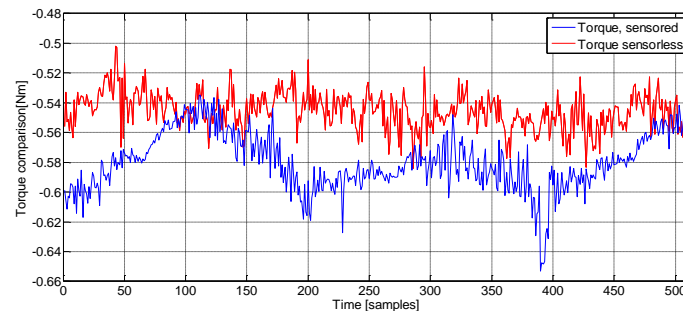


Fig. 3 Experimental results for comparison of electromagnetic torque with sensor and sensorless control.

From figure 3 it is clear that electromagnetic torque during sensorless operation is more stable and has fewer ripples. The ripple’s amplitude for torque during sensorless operation is reduced up to 50% of ripple’s amplitude of torque during sensor operation. This is not an isolated fact, which occurs accidentally. The replacing of encoder with soft block SMO, “confront” directly one of the receivers of EMI noises, e.g. position sensor. In general, the “first line of defense” is to suppress the emission as much as possible at the source, but it is a valid strategy to make the control system “deaf” for a part of EMI noises.

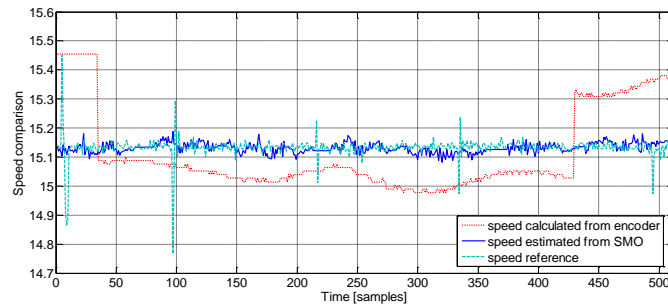


Fig. 4 Experimental results for comparison of speed response in steady state with sensor and sensorless control during rated speed regime.

Figure 4 shows the experimental results for speed response at steady state for both sensor and sensorless operation near rated speed. The taken results show very clear that sensorless operation provide a smooth speed control almost equal to reference speed. Compared with speed response of sensor operation, the accuracy of speed estimation during sensorless operation is very high and speed error is approximately zero. So, the rotor speed reflects a great benefit in using a sensorless scheme for vector control of IPMSM from EMI noises point of view.

Another important quantity for Field Oriented Control algorithm is direct current i_d . In order to verify the validity of our strategy, we have to check the effect expressed in results for other important quantities in Field Oriented Control like rotor speed and direct current i_d . Currents i_d and i_q , are variables calculated by Clarke and Park vector transformations of digitalized real currents flowing into stator of IPMSM, sensed with Hall Effect sensors and digitalized with ADC converter. The direct current i_d is a flux-producing component that during execution of the FOC algorithm, is forced to zero in order to achieve the maximum torque production for a given stator current. So, being this very important, the results for current i_d during sensor and sensorless operation are put together in figure 5, where it is clearly shown that amplitude of ripples for current i_d is reduced by 50% during sensorless operation.

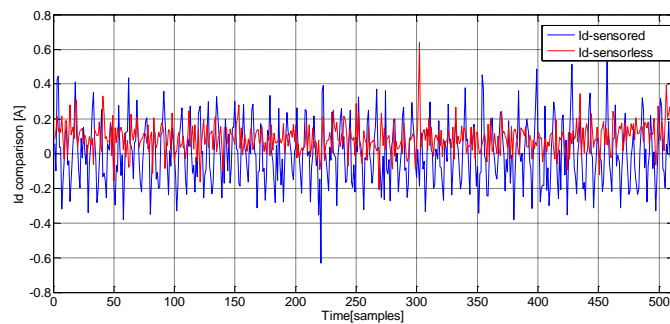


Fig. 5 Experimental results showing comparison between direct current i_d in sensed and sensorless control.

The sensorless drive systems based on state observers, suffer from the un-observability in the area of very low speed.

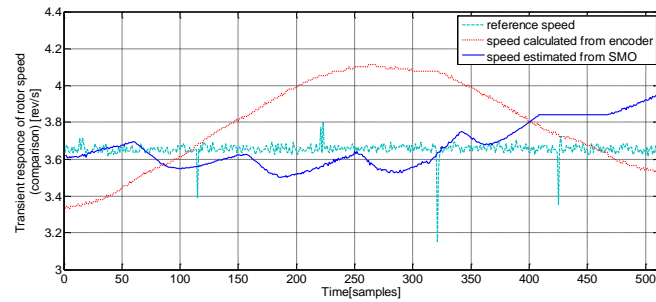


Fig. 6 Experimental results for comparison of speed response in steady state during very low speed regime with sensor and sensorless control.

Since this is the lower boundary of functionality of observer, where all quantities tend to be uncontrollable, it seems to be useful to compare the speed responses for both sensor and sensorless operation. Figure 6 shows a better behavior of observer at very low speed than using the encoder. The speed fluctuations are less than 50% during sensorless operation.

The transient response is quite important when analyzing the behavior of a device. Figure 7 show the transient response for torque during sensor and sensorless operation. It is clearly shown that sensorless operation has a smaller overshoot and need less time (the half) to stabilize.

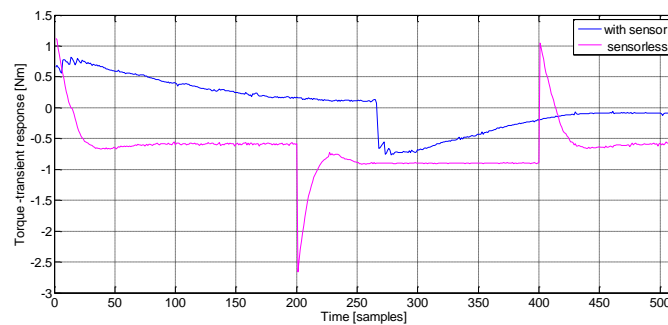


Fig. 7 Experimental results for comparison of transient response for torque during sensor and sensorless operation.

Figure 8 shows the transient responses for speed during sensor and sensorless operation. It is clearly shown that sensorless operation has a smaller overshoot (approximately 7%) and need almost the same time to be stabilized.

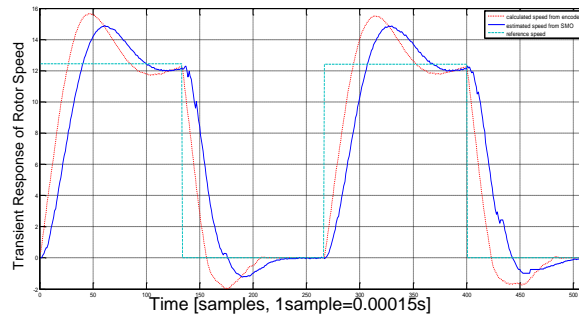


Fig. 8 Experimental results for comparison of transient response for rotor speed during sensor and sensorless operation.

The Fig. 9 show the results for angle estimation during sensorless operation by Sliding Mode Observer. The accuracy of angle estimation is crucial for control performance because that angle estimated by SMO block is used to calculate the rotor speed and to realize vector transformations of Clarke and Park in order to generate the right value of voltage by SVPWM block.

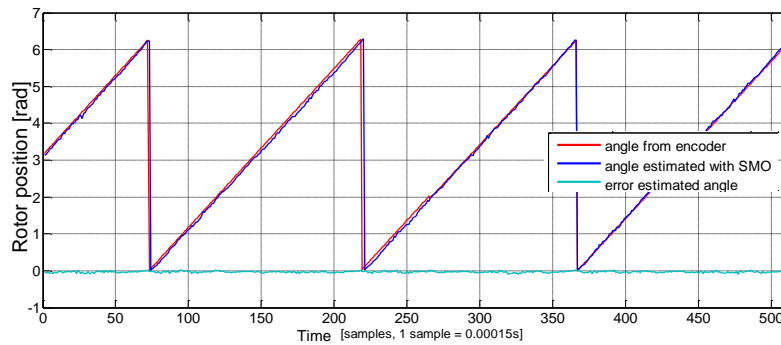


Fig. 9 Experimental results for rotor position estimation by SMO and encoder.

As a summary of experimental results, one may conclude that elimination of one of receptors of EMI noises (encoder) make the control system less susceptible to them. This strategy, although ranked third, is very useful in achieving a better overall performance of control system.

An accurate view of all results confirms that using the sensorless mode of operation has a lot of benefits. This kind of nonlinear control (the sliding mode), “suffer” from chattering phenomena while implementation in real time control of AC drives and IPMSM drives too. It is obvious that the chattering is overlapped to speed and torque ripples, resulting in a worse situation. But the encoder, is the most susceptible hardware part of the drive by EMI, and replacing that hardware with a software, the SMO block,

reduce the possibility to effect the drive operation. Experimentally, result that the torque ripples are reduced in total up to 50%.

5. CONCLUSIONS

The paper presents main problems of practical implementation of sensorless FOC of an IPMSM. Electromagnetic distortions have pernicious influence on the calculations performed in control unit as well as for the operation of absolute encoder. Eliminating one of the sufferers from EMI noises, by replacing it with a Sliding Mode Observer, provide a noticeable improvement in response of speed and torque in the control system. This improvement is reflected in decreasing effect of EMI, higher efficiency, less vibrations, and better overall performance. Different experiments were performed on sensor and sensorless FOC and measurements of currents, torque, rotor speed and currents are compared.

Acknowledgement: *This paper presents a part of the work supported by the research program of ERASMUS MUNDUS/Basileus IV (2013-2014), in Laboratories of Department of Mechatronics, Faculty of Electrical Engineering, University of Ljubljana, Slovenia..*

REFERENCES

- [1] L. Dharmo, A. Spahiu, M. Nemeč, V. Ambrožič, "Electromagnetic Interference Reduction by Using Sensorless FOC of IPMSM with PICCOLOF28069 Controlstick", In Proceedings of the Extended Abstracts of the 13th International Conference on Applied Electromagnetics (IEEC 2017), Niš, Serbia, 2017, pp. 69.
- [2] B. K. Bose, "Power Electronics And Motor Drives: Advances and Trends". USA: Elsevier, 2006.
- [3] Y. Xu, Q. Yuan, J. Zou, Y. Li, "Analysis of triangular periodic carrier frequency modulation on reducing electromagnetic noise of permanent magnet synchronous motor", *IEEE Trans. Magn.*, vol. 48, no. 11, pp. 4424-4427, 2012.
- [4] R. L. Kirlin, S. Kwok, S. Legowski, A. M. Trzynadlowski, "Power spectra of a PWM inverter with randomized pulse position", *IEEE Trans. Power Electron.*, vol. 9, no. 5, pp. 463-472, 1994.
- [5] K. S. Kim, Y. G. Jung, Y. C. Lim, "A new hybrid random PWM scheme", *IEEE Trans. Power Electron.*, vol. 24, no. 1, pp. 192-200, 2009.
- [6] S. Kaboli, J. Mahdavi, A. Agah, "Application of random PWM technique for reducing the conducted electromagnetic emissions in active filters", *IEEE Trans. Ind. Electron.*, vol. 54, no. 4, pp. 2333-2343, 2007.
- [7] A. M. Hava, E. Un, "Performance analysis of reduced common-mode voltage PWM methods and comparison with standard PWM methods for three-phase voltage-source inverters", *IEEE Trans. Power Electron.*, vol. 24, no. 1, pp. 241-252, 2009.
- [8] Y. C. Lim, S. O. Wi, J. N. Kim, Y. G. Jung, "A pseudorandom carrier modulation scheme", *IEEE Trans. Pow. Electron.*, vol. 25, no. 4, pp. 797-805, 2010.
- [9] J.-Y. Chai, Y.-H. Ho, Y.-C. Chang, C.-M. Liaw, "On acoustic-noise reduction control using random switching technique for switch mode rectifiers in PMSM drive", *IEEE Trans. Ind. Electron.*, vol. 55, no. 3, pp. 1295-1309, 2008.
- [10] H. Khan, E. Miliani, K. E. K. Drissi, "Discontinuous random space vector modulation for electric drives: A digital approach", *IEEE Trans. Power Electron.*, vol. 27, no. 12, pp. 4944-4951, 2012.
- [11] K. T. Chau, Z. Wang, "Chaos in Electric Drive Systems-Analysis, Control and Application". Singapore: Wiley, 2011.
- [12] H. Li, Y. Liu, J. Lu, T. Zheng, X. Yu, "Suppressing EMI in power converters via chaotic SPWM control based on spectrum analysis approach", *IEEE Trans. Ind. Electron.*, vol. 61, no. 11, pp. 6128-6136, 2014.
- [13] Z. Wang, K. T. Chau, C. H. Liu, "Improvement of electromagnetic compatibility of motor drives using chaotic PWM", *IEEE Trans. Magn.*, vol. 43, pp. 2612-2614, 2007.

- [14] Z. Zhang, K. T. Chau, Z. Wang, W. Li, "Improvement of electromagnetic compatibility of motor drives using hybrid chaotic pulse width modulation", *IEEE Trans. Magn.*, vol. 47, no. 10, pp. 4018-4021, 2011.
- [15] C.R. Paul " *Introduction to Electromagnetic Compatibility*", Second Edition, John Wiley & Sons, Inc., Hoboken, New Jersey, 2006.
- [16] Dabi, J. Zare, F. Ledwich, G. Ghosh, A., "Leakage current and common mode voltage issues in modern AC drive systems," Power Engineering Conference, 2007. AUPEC 2007. Australasian Universities, pp.1-6, 9-12 Dec. 2007.
- [17] E. Haseloff, "Printed Circuit Board Layout for Improved Electromagnetic Compatibility", Texas Instruments 1996.